JPL Publication 89-11

A Novel Multistage Estimation of the Signal Parameters of a Possibly Data-Modulated Sinusoid Under Very High Dynamics

R. Kumar

May 1, 1989

Prepared for

U.S. Air Force Systems Command
Armament Division

Through an agreement with

National Aeronautics and
Space Administration

by

Jet Propulsion Laboratory
California Institute of Technology
Pasadena, California

JPL Publication 89-11

A Novel Multistage Estimation of the Signal Parameters of a Possibly Data-Modulated Sinusoid Under Very High Dynamics

R. Kumar

May 1, 1989

Prepared for

U.S. Air Force Systems Command
Armament Division

Through an agreement with

National Aeronautics and
Space Administration

by

Jet Propulsion Laboratory
California Institute of Technology
Pasadena, California

The research described in this publication was carried out by the Jet Propulsion Laboratory, California Institute of Technology, and was sponsored by the United States Air Force Systems Command through an agreement with the National Aeronautics and Space Administration.

ABSTRACT

This publication presents a novel multistage estimation scheme for estimating the parameters of a received carrier signal possibly phase-modulated by unknown data, and experiencing very high Doppler, Doppler rate, etc. Such a situation arises, for example, in the case of Global Positioning Systems (GPS) where the signal parameters are directly related to the position, velocity, acceleration and jerk of the GPS receiver.

In the proposed multistage scheme, the first stage estimator operates as a coarse estimator resulting in higher rms estimation errors but with a relatively small probability of the frequency estimation error exceeding one-half of the sampling frequency (an event termed cycle slip). The second stage of the estimator operates on the error signal available from the first stage, refining the overall estimates, and in the process also reduces the number of cycle slips. The first stage algorithm is selected to be a modified least squares algorithm operating upon the differential signal model and referred to as differential least squares (DLS). This estimation stage provides relatively coarse estimates of the frequency and its derivatives. The second algorithm is simply an extended Kalman filter (EKF) which also yields the estimate of the phase along with a more refined estimate of frequency as well.

A major advantage of the proposed algorithm is a reduction in the threshold on received carrier power-to-noise power spectral density ratio (CNR) as compared to the threshold achievable by either of these algorithms alone. In fact, it appears from the simulations that for the case of an unmodulated carrier, the proposed scheme achieves the same threshold as for an almost exact and computationally intensive implementation of the maximum likelihood estimator (MLE). For the case when data modulation is present, the proposed scheme provides an improvement of about 6 dB in terms of CNR compared to an earlier MLE scheme reported in the literature. The overall complexity of the algorithm is about two times the complexity of a third-order Kalman filter or a single fourth-order EKF.

CONTENTS

1. INTRODUCTION

The problem of estimating the parameters of a received quasi-sinusoidal signal in the presence of noise occurs in diverse scientific and engineering disciplines [1-15]. The signal parameters of interest are usually the phase, frequency and frequency derivatives which are varying with time. The estimation problem becomes considerably more difficult if the received carrier is modulated by unknown data while simultaneously experiencing very high Doppler and Doppler rate. Such situations occur, for example, in the cases of Global Positioning System (GPS) receivers and NASA deep space communication links under high spacecraft dynamics.

In a previous publication [7], an estimator structure based on the maximum likelihood estimation (MLE) of code delay and Doppler frequency over a single data-bit period has been proposed and analyzed for the GPS applications. This scheme estimates Doppler frequency (assumed constant) over successive intervals of bit periods, followed by a Kalman filter tracking Doppler frequency and frequency rate. The scheme does not involve the carrier phase estimation. For the dynamic trajectories simulated in [7], the approximate ML estimator performance exhibited a threshold of about 30 dB-Hz in terms of the received carrier power-to-noise power spectral density ratio (P/N_0), below which rapid performance deterioration occurred.

For GPS applications, an alternative scheme has been proposed [8] wherein a parallel (non-dynamic) link is established between the GPS satellites and a control ground receiver for the purpose of communicating the data to the ground receiver. The ground receiver simultaneously receives the frequency-translated version of the GPS receiver signal and removes the data modulation from this dynamic signal. Such an effectively demodulated signal is then processed by the estimation algorithm to obtain the desired signal parameter estimates. There are several estimation schemes in the literature for this problem. See for example [9-14].

More recently in [9] a scheme for simultaneous detection and estimation has been

proposed. This scheme is based upon first estimating the received signal's local (data dependent) parameters over two consecutive bit periods, followed by the detection of a possible jump in these parameters. The presence of the detected jump signifies a data transition which is then removed from the received signal. This effectively demodulated signal is then processed to provide the estimates of the global (data independent) parameters of the signal related to the position, velocity, etc., of the receiver. A key feature of this scheme is that to a certain extent the data detection is independent of the acquisition of the phase or frequency of the received carrier signal in contrast to the conventional decision-directed phase-locked loop receivers. In these latter receivers, the data detector is an integral part of the loop and depends upon the acquisition of the carrier phase and/or frequency. Thus, under low CNR and/or high dynamic conditions, the loop may not acquire lock or frequently lose it during tracking. From the simulations of [9], it is seen that the scheme offers very significant improvement in terms of the required CNR over the AMLE algorithm of [7]. The detection-estimation scheme of [9] has a computational complexity about three times that of a single extended Kalman filter.

In this publication we propose an alternative scheme for the estimation of the signal parameters applicable for both the cases of unmodulated carrier and when the signal is phase-modulated by unknown data. The proposed scheme is somewhat simpler than that of [9] in that it is not essential to detect the data modulation explicitly. Basically, the proposed algorithm involves an appropriate modification of the DLS scheme of [11] so as to apply the algorithm to the case of unknown data modulation. As discussed in [11], if the DLS technique is applied with the Nyquist sampling of the received signal, there is expected a loss in performance compared to the optimum achievable performance. The techniques of [11] propose oversampling and cyclic sampling strategies to avoid such a loss. In the present example of GPS application, we sample at Nyquist rate and propose an alternative method to keep the overall performance close to optimum. The

technique proposed here consists of a multistage procedure wherein the parameters of the signal are estimated in more than one stage. First, the parameters are estimated by an algorithm like DLS which has a low threshold on CNR but with possibly higher rms estimation errors. Then an error signal whose parameters are equal to the difference between the true parameters and the above estimates is processed by another algorithm to estimate these error signal parameters. Since the error signal involves much smaller dynamics, the second algorithm can have smaller bandwidth resulting in a smaller estimation error. In principle, this procedure can be repeated any number of times with successive algorithms having progressively lower bandwidths.

In this publication we confine ourselves to two stages of recursion and apply a third-order extended Kalman filter algorithm for the second recursion. It is expected from such an estimation structure that the overall algorithm would have both smaller threshold and a smaller estimation error compared to either algorithm operating by itself. Indeed, this is borne out by simulations presented in the publication. Thus, for the case of no data modulation, whereas the threshold on SNR is about 1.5 dB lower than the extended Kalman filter, the estimation errors are only marginally higher than for the third-order EKF alone. The threshold achieved is in fact the same as that achieved for a nearly exact implementation of the maximum-likelihood estimator (MLE). It is also noted that the threshold achieved by the proposed scheme is about 3 dB lower than conventional cross product AFC (CPAFC) loops and phase-locked loops [14], whereas the rms error is less than one-half of that obtained by CPAFC. The rms error is marginally higher than EKF due to the non-optimal sampling used in the DLS algorithm.

For the case of data modulation, we compare our results with those of [7], where analysis and simulations are presented on the performance of Fast Fourier Transform (FFT) based MLE algorithm. In [7], the trajectories of the GPS signals have somewhat less severe dynamics compared to those considered in this publication. In terms of threshold on CNR, the proposed scheme of this publication exhibits a threshold of 24

dB-Hz compared to about 30 dB-Hz reported in [7], thus providing an improvement of about 6 dB. In terms of the rms frequency estimation errors, at a 30 dB-Hz CNR, the scheme of [7] provides a rms range rate error of about 6 m/s compared to an error of less than 2 m/s achieved in this publication. There is also a very significant improvement in terms of the rms position estimation error. At about 30 dB-Hz an rms error of 1 meter is reported in [7], compared to about 0.25 meter obtained by the proposed algorithm. It may also be remarked that in the previous scheme, pseudo-random codes with rate 10.23 MHz are needed for the purpose of range measurements, thus requiring a zero-crossing channel bandwidth in excess of 20 MHz. The proposed scheme, on the other hand, extracts the range information from the carrier signal itself and thus needs a bandwidth equal to only a fraction of 1 MHz.

2. THE RECEIVER CONFIGURATION

We consider the problem of estimating the high dynamic phase process $\Theta_I(t)$ of the desired signal $s_I(t)$ observed in the presence of an additive narrow-band noise process $v_I(t)$ as

$$\begin{aligned} r_I(t) &= s_I(t) + v_I(t) \\ &= ASin(\omega_c t + \Theta_I(t) + \pi D(t)) + v_I(t) \end{aligned} \tag{1}$$

In (1) ω_c is the received signal carrier frequency in the absence of any dynamics and $D(t)$ is a binary digital waveform taking on the possible values of 0 or 1. In the case of a Global Positioning System (GPS) receiver, the process $\Theta_I(t)$ arises from the receiver dynamics, and over a sufficiently small estimation period,

$$\Theta_I(t) = \theta_{I0} + \omega_{I0}t^1 + \gamma_{I0}t^2 + \delta_{I0}t^3 \tag{2}$$

for some unknown parameter vector $\psi_{I0} = [\theta_{I0}\ \omega_{I0}\ \gamma_{I0}\ \delta_{I0}]'$. In a somewhat simpler version of the problem, the data modulation $D(t)$ is either absent or is assumed known and thus can be eliminated from (1). In the sequel both of these cases would be treated in some detail.

In the first instance we only estimate the parameters related to the frequency and its derivatives using the DLS algorithm. For this purpose, the received signal $r_I(t)$ is quadrature demodulated by the voltage-controlled oscillator (VCO) signal $s_L(t)$ as shown in Figure 1. We assume that the input to the VCO is a signal which is an appropriate quadratic function of time t resulting in its instantaneous phase $\Theta_L(t)$ in (3) below.

$$\begin{aligned} s_L(t) &= 2Cos(\omega_c t + \Theta_L(t)) \\ \Theta_L(t) &= \theta_{L0} + \omega_{L0}t + \gamma_{L0}t^2 + \delta_{L0}t^3 \end{aligned} \tag{3}$$

for some constant vector $\psi_{L0} = [\theta_{L0}\ \omega_{L0}\ \gamma_{L0}\ \delta_{L0}]'$. The sampled version of the in-phase and quadrature components of the demodulated signal are given by

$$
\begin{aligned}
y(k) &= ASin(\Theta(k) + \pi D(k)) + v_i(k) \\
z(k) &= ACos(\Theta(k) + \pi D(k)) + v_q(k) \quad ; k = 1, 2, \ldots, N
\end{aligned}
\tag{4}
$$

where

$$
\Theta(k) = \Theta_I(k) - \Theta_L(k) = \theta_0 + \omega_0 k T_s + \gamma_0 (k T_s)^2 + \delta_0 (k T_s)^3
$$

$$
\psi_0 \triangleq \psi_{I0} - \psi_{L0} = [\theta_0 \ \omega_0 \ \gamma_0 \ \delta_0]'
$$

and ψ_0 is the parameter vector characterizing the error signal to be estimated, with T_s denoting the sampling interval. In (4) $v_i(k)$ and $v_q(k)$ represent the sampled in-phase and quadrature components of the bandpass noise process $v_I(k)$. The parameter vector ψ_0 is estimated by the Differential Least Squares (DLS) algorithm of [11], as described in the following section.

3. DIFFERENTIAL LEAST SQUARES (DLS) ALGORITHM

Consider first the problem of estimating the unknown parameters ω_0, γ_0 and δ_0 from the measurement (4) for the case of no data modulation, i.e. when $D(k) \equiv 0$. Following [11] we expand $Sin(\Theta(t))$ in a Taylor series around $t_{k-1} = (k-1)T_s$ to obtain

$$Sin(\Theta(t)) = Sin(\Theta(k-1)) + T\dot{\Theta}(k-1)Cos(\Theta(k-1)) + \dots \tag{5}$$

with a similar expansion for $Cos(\Theta(t))$. For small $(t - t_{k-1})$, the series in (5) may be approximated by the first two terms and from (4) one obtains the following differential signal model with $\tau_k = (k - \frac{1}{2})T_s$:

$$\begin{aligned} y_d(k) &\triangleq y(k) - y(k-1) = T_s(\omega_0 + 2\gamma_0\tau_k + 3\delta_0\tau_k^2)z(k-1) + \xi_i(k) \\ z_d(k) &\triangleq z(k) - z(k-1) = -T_s(\omega_0 + 2\gamma_0\tau_k + 3\delta_0\tau_k^2)y(k-1) + \xi_q(k) \end{aligned} \tag{6}$$

where

$$\begin{aligned} \xi_i(k) &\triangleq v_i(k) - v_i(k-1) - T_s(\omega_0 + 2\gamma_o\tau_k + 3\delta_0\tau_k^2)v_q(k-1) \\ \xi_q(k) &\triangleq v_q(k) - v_q(k-1) + T_s(\omega_0 + 2\gamma_0\tau_k + 3\delta_0\tau_k^2)v_i(k-1) \end{aligned} \tag{7}$$

The measurement model (6) may be rewritten in the following standard form as in [11]:

$$Z_d(k) = H'(k)\beta + \xi(k) \quad ; k = 1, 2, \dots N \tag{8}$$

where

$$\begin{aligned} \beta' &= [\omega_0 \quad 2\gamma_0 \quad 6\delta_0] \\ H'(k) &= \begin{bmatrix} T_s z(k-1) & T_s\tau_k z(k-1) & 0.5\,T_s\tau_k^2 z(k-1) \\ -T_s y(k-1) & -T_s\tau_k y(k-1) & -0.5\,T_s\tau_k^2 y(k-1) \end{bmatrix} \\ Z_d'(k) &= [y_d(k)\ z_d(k)] \quad ; \xi'(k) = [\xi_i(k)\ \xi_q(k)] \end{aligned} \tag{9}$$

The parameter vector β in (8) is now estimated by an exponential data-weighted least squares algorithm in a recursive or nonrecursive form (Kalman filter). In its nonrecursive form the estimate of β obtained on the basis of N measurements and denoted by $\hat{\beta}(N)$ is given by

$$\hat{\beta}(N) = \{\sum_{j=1}^{N} H(j)H'(j)\lambda^{N-j}\}^{-1}\{\sum_{j=1}^{N} H(j)Z_d(j)\lambda^{N-j}\} \tag{10}$$

where λ is some appropriate weighting coefficient with $0 < \lambda < 1$. An equivalent recursive form of (10) is the following algorithm:

$$\begin{aligned}
&\hat{\beta}(k) = \hat{\beta}(k-1) + L(k)\epsilon(k) \\
&L(k) = P(k-1)H(k)[\lambda I + H'(k)P(k-1)H(k)]^{-1} \\
&P(k) = \{P(k-1) - P(k-1)H(k)[\lambda I + H'(k)P(k-1)H(k)]^{-1}H'(k)P(k-1)\}/\lambda \\
&\epsilon(k) = Z_d(k) - H'(k)\hat{\beta}(k-1) \quad ; k = 1, 2, \ldots, N
\end{aligned} \tag{11}$$

Note that the matrix to be inverted in (11) is only a (2 × 2) matrix. In an alternative but equivalent form one may process the scalar measurements $y_d(k)$, $z_d(k)$ sequentially instead of working with vector measurement $Z_d(k)$. Moreover, the matrix $P(k)$ of (11) with $k = N$ is the same as the matrix inverse in (10), i.e.,

$$P^{-1}(k) = \sum_{j=1}^{k} H(j)H'(j)\lambda^{k-j} \tag{12}$$

Alternatively, the matrix $P^{-1}(k)$ may be written as

$$P^{-1}(k) = \sum_{j=1}^{k} \lambda^{k-j}\{z^2(j) + y^2(j)\}B_j T_s^2; B_j \triangleq \begin{bmatrix} 1 & \tau_j & \tau_j^2 \\ \tau_j & \tau_j^2 & \tau_j^3 \\ \tau_j^2 & \tau_j^3 & \tau_j^4 \end{bmatrix} \tag{13}$$

and thus the matrix $P(k)H(k)$ required in the update of $\beta(k)$, and equal to $L(k)$ in (11) may be approximated by

$$\begin{aligned}
&P(k)H(k) \cong \chi(k)[z(k) \ - y(k)] \\
&\chi'(k) = (\sum_{j=1}^{k} \lambda^{k-j} B_j)^{-1}(A^2 + \sigma_v^2)^{-1}[1 \quad \tau_k \quad \tau_k^2]' T_s^{-1}
\end{aligned} \tag{14}$$

where

$$E[v_i^2] = E[v_q^2] = \frac{1}{2}\sigma_v^2 \quad ; \quad E[z^2(j) + y^2(j)] = A^2 + \sigma_v^2$$

In (14) the vector $\chi(k)$ is data independent and thus could be precomputed for $k = 1,2,\ldots,N$ for computational simplification of (11). Similarly, in the implementation of (10), the first matrix may be replaced by the data independent matrix $(\sum_{j=1}^{N} \lambda^{N-j} B_j)(A^2 + \sigma_v^2)T_s^2$.

Modified Least Squares Algorithm

If the noise $\xi(k)$ in the signal model (8) were white, then the estimate $\hat{\beta}(N)$ obtained from the algorithm (10) or (11) would approach 0 as $N \to \infty$, if one ignores the approximation made in arriving at model (8) and λ is selected equal to 1. However, as the noise $\xi(k)$ in the model (8) is colored, there would be considerable bias in the parameter estimates under low to medium signal-to-noise ratios. To reduce such a bias or possibly eliminate it we propose the following simple modification. If the instantaneous frequency $\omega(\tau_k)$ at time τ_k given by $(\omega_0 + 2\gamma_0\tau_k + 3\delta_0\tau_k^2)$ appearing in (7) is small compared to $1/T_s$, then the noise vector $\xi(k)$ is equal to $v(k) - v(k-1)$ where $v(k) \triangleq [v_i(k)v_q(k)]'$. This situation may be depicted by Figure 2a.

To eliminate the bias, the noise $\xi(k)$ must be whitened by passing through the transfer function $(1-z^{-1})^{-1}$ as shown in Figure 2b. The least squares algorithm is, in general, nonlinear and time-varying. However, if we assume that the algorithm in (11) asymptotically approaches a time-invariant system, then under such an assumption, one may interchange the least squares algorithm with the transfer function $(1-z^{-1})^{-1}$ to arrive at Figure 2c. This, of course, corresponds to post-averaging the least squares estimates. Such a simple procedure provides very significant improvement in the estimates when the signal-to-noise ratio is low. In the simulations of the next section, the infinite time averaging is replaced by an exponentially data-weighted averaging to take into account the time variation of the parameters to be estimated. In Figures 2b and 2c, $\hat{\beta}_{uB}$ denotes an unbiased estimate of β.

DLS Algorithm in the Data Modulation Case

In this case the data samples $D(k)$ in the signal model (4) may take possible values ± 1 and the received signal may equivalently be written as

$$\begin{aligned} y(k) &= D(k)ASin(\Theta(k)) + v_i(k) \\ z(k) &= D(k)ACos(\Theta(k)) + v_q(k) \quad ; k = 1, 2, \ldots, N \end{aligned} \tag{15}$$

Thus, as may be easily verified, over any bit interval T_b, where $D(k)$ remains constant, the differential model (6) remains valid irrespective of the value of $D(k)$. The model (6), however, is not applicable for those samples which lie on the bit boundaries, i.e., when $y(k)$ and $y(k-1)$ lie in different bit intervals. A simple modification of the algorithm to take care of the data modulation case is to simply discard such differential samples. If the number of samples M over any bit period is fairly large, this would incur a negligible loss in the effective signal-to-noise ratio compared to the case of no data modulation. In fact, such a loss is simply equal to $10\,log_{10}(1-\frac{1}{M})\,dB$ which is 0.45 dB for $M = 10$. This is corroborated by the simulations of the next section.

Estimation of Time-Varying Parameters

In the signal model considered above we have assumed that the input signal parameter vector ψ_{I0} is either a constant or a slowly varying function of time. However, in practice this may be the case only over relatively short intervals of time, but there may be large variations in ψ_{I0} over a comparatively large observation period. To take into account such a variation and to ensure that the instantaneous difference frequency $\Omega(t) \triangleq \frac{d}{dt}\Theta(t)$ (the sampled version of $\Theta(t)$ given in (4)) remains within the low-pass filter-pass band of Figure 1, the parameter vector ψ_{L0} generating the instantaneous frequency of the VCO is updated at regular intervals of $T = NT_s$ sec for some integer N. The parameter vectors ψ_I, ψ_{L0} and ψ_0 would change their values at intervals of T sec, assuming that the value of N is selected to be sufficiently small so that the variation in ψ_I over any T sec interval is small. Denoting by $\theta_{L0}(T+), \omega_{L0}(T+)$, etc., the values of reference

oscillator parameters just after the update at time T, we have that

$$\begin{aligned}
\theta_{LO}(T+) &= \Theta_{LO}(T-) \\
\omega_{LO}(T+) &= \Omega_{LO}(T-) + \hat{\omega}_0(0/T) + 2T\hat{\gamma}_0(0/T) + 3T^2\hat{\delta}_0(0/T) \\
\gamma_{LO}(T+) &= \Gamma_{LO}(T-) + 3T\hat{\delta}_0(0/T) \\
\delta_{LO}(T+) &= \Delta_{LO}(T-) + \hat{\delta}_0(0/T)
\end{aligned} \tag{16}$$

In equation (16), $\Theta_{LO}(T-)$, $\Omega_{LO}(T-)$, etc., represent the oscillator instantaneous phase, frequency, etc., just before the correction and the remaining terms on the right-hand side of (16) represent the correction made on the basis of the estimation algorithm. Thus,

$$\begin{aligned}
\Theta_{LO}(T-) &= \theta_{LO}(0+) + \omega_{LO}(0+)T + \gamma_{LO}(0+)T^2 + \delta_{LO}(0+)T^3 \\
\Omega_{LO}(T-) &= \omega_{LO}(0+) + 2\gamma_{LO}(0+)T + 3\delta_{LO}(0+)T^2 \\
\Gamma(T-) &= \gamma_{LO}(0+) + 3T\delta_{LO}(0+) \\
\Delta_{LO}(T-) &= \delta_{LO}(0+)
\end{aligned} \tag{17}$$

Note that in (16) there is no correction in the oscillator phase as the DLS algorithm does not provide the phase estimate. In equation (16), $\hat{\omega}_0(0+/T)$ denotes the estimate of parameter $\omega_0(0+)$ obtained on the basis of measurements up to time T. Since there is no step change in the oscillator phase, the sampled measurements $y(N)$ and $z(N)$ at the demodulator output are the same with or without a correction at the instance NT_s. However, the subsequent measurements $y(N+j)$ and $z(N+j)$ are now expressed with respect to the new parameter vector $\psi_0(T+) = [\theta_0(T+)\ \omega_0(T+)\ \gamma_0(T+)\ \delta_0(T+)]' \triangleq \psi_{IO}(T+) - \psi_{LO}(T+)$ as in (18) below.

$$\begin{aligned}
y(N+j) &= ASin(\Theta(N+j)) + v_i(N+j) \\
z(N+j) &= ACos(\Theta(N+j)) + v_q(N+j) \quad ; j = 1, \ldots, N \\
\Theta(N+j) &= \theta_0(T+) + \omega_0(T+)jT_s + \gamma_0(T+)(jT_s)^2 + \delta_0(T+)(jT_s)^3
\end{aligned} \tag{18}$$

The last three elements of the vector $\psi_0(T+)$ will be zero if there is no change in the input signal parameters over the T sec interval and the estimate of $\psi_0(0+)$ is obtained

with zero estimation error. We thus set the a-priori estimate of the vector $\psi_0(T+)$ equal to 0 and apply the DLS algorithm to estimate $\psi_0(T+)$ on the basis of observations $\{y(N+j), z(N+j); j = 1, \ldots, N\}$. The measurement model is obtained by simply replacing the index k by $k+N$ in $y(k), z(k), \xi_i(k), \xi_q(k)$ in equations (6-9) but with $\tau_k = (k - \frac{1}{2})T_s$ as before (corresponding to a shift in time reference).

In the estimation of $\psi_0(T+)$ via the recursive algorithm (11) with the index $k = N+1, \ldots, 2N$, the "initial" covariance matrix $P(N+1)$ is obtained as

$$P(N+1) = \lambda F P(N) F' + Q \tag{19}$$

where

$$F \triangleq \begin{bmatrix} 1 & 2T & 3T^2 \\ 0 & 1 & 3T \\ 0 & 0 & 1 \end{bmatrix}$$

and the matrix Q represents the uncertainty introduced due to the change in the input process parameters over the interval of T sec. Specifically, the last diagonal element of Q represents the variance of the change in the parameter 6δ (equal to the second derivative of frequency and related to the jerk of the physical trajectory) over the interval T. The above procedure is then extended in a straightforward manner to the subsequent update intervals. The estimates of input signal phase and frequency at time instances $\ell T+$ are then simply given by $\theta_{L0}(\ell T+)$ and $\omega_{L0}(\ell T+)$ respectively for $\ell = 0, 1, 2, \ldots$.

4. MULTISTAGE ESTIMATION

We note that most of the phase and frequency estimation schemes can be represented as in Figure 3a. The block representing the VCO correction signal could be any recursive or semi-recursive algorithm including an EKF or DLS algorithm, and the VCO update interval may be some integer multiple of sampling period T_s. Figure 3b depicts an equivalent and a more compact representation of the estimation scheme. An important observation made from figure 3b is that along with the estimate of the input phase process $\Theta_I(t)$ represented by $\Theta_L(t)$, there is also available a pair of signals, $(ASin\tilde{\Theta}(t),\ ACos\tilde{\Theta}(t))$ dependent upon the estimation error $\tilde{\Theta}(t) = \Theta_I(t) - \Theta_L(t)$. These error signals have exactly the same form as the signals at the input to the estimator. Moreover, the additive noise associated with these signals has statistics identical with the statistics of the noise at the input to the estimator. Therefore, this leads to the clear possibility of estimating the error signal $\tilde{\Theta}(t)$ in a way similar to the estimation of $\Theta_I(t)$. In fact, the procedure can at least in principle be repeated any number of times as shown in Figure 4. It may also be noted that the first estimation stage (Figure 3a) requires a VCO for down conversion as the actual input to this stage is at rf frequency ω_c. However, subsequent estimator stages generate the error signals by simple baseband computations. For example, in the discrete-time version of the estimation procedure, the signal at the output of estimation stage m may simply be computed as

$$\begin{aligned} y^m(k) &= y^{m-1}(k)Cos(\hat{\Theta}^{m-1}(k-1)) - z^{m-1}(k)Sin(\hat{\Theta}^{m-1}(k-1)) \\ z^m(k) &= y^{m-1}(k)Sin(\hat{\Theta}^{m-1}(k-1)) + z^{m-1}(k)Cos(\hat{\Theta}^{m-1}(k-1)) \quad ;m = 2,3,\ldots n \end{aligned} \tag{20}$$

Note that $\tilde{\Theta}(t), \tilde{v}_i(t)$ and $\tilde{v}_q(t)$ of Figure 3b are respectively equal to $\Theta^1(t)$, $v_i^1(t)$, $v_q^1(t)$ of Figure 4. The refined estimate of $\Theta_I(k)$ is then simply given by

$$\hat{\hat{\Theta}}_I(k) = \Theta_L(k) + \hat{\Theta}^1(k) + \cdots + \hat{\Theta}^n(k) \tag{21}$$

The advantage of such a recursive estimation procedure is that the overall threshold

in terms of the required CNR for the multistage estimator can be made much smaller than a single stage estimator, especially in situations involving high dynamics. In a single stage estimator, due to the high dynamics involved, the process parameters may be assumed to remain constant only over short intervals of time. Thus, the estimator is forced to use a relatively large noise bandwidth (shorter averaging period), resulting in large errors in the phase and/or frequency estimates. If the estimation errors are outside the region over which the error model (linear) assumed for the estimator remains valid, the estimator is said to be working below threshold or in the out-of-lock condition. In this condition the estimation errors can be several orders of magnitude higher compared to the operation above threshold. In a multistage estimator environment this difficulty can be circumvented by successive reduction of the dynamics (the estimation errors due to dynamics) at the output of consecutive estimator stages and by averaging the signal over progressively longer intervals (and thus progressively reducing the effect of noise) over which the process parameters remain nearly constant. In this estimation structure, none of the individual stages (except the last one) need necessarily operate above its threshold. For the convergence of the overall estimator, one only requires that the estimates are made in the right direction (estimation errors do not exceed the parameters to be estimated in some average sense). The proposed estimation scheme may look familiar if one compares it with the standard practice of weighing wherein the estimation proceeds from a coarse estimate to a successively refined one thereby achieving high estimation accuracy with a comparatively less complex setup. Similar approaches, variously termed method of successive approximation, method of sieves, and so on, are also common in various mathematical disciplines including theory of differential equations, probability theory, etc.

5. RECURSIVE DLS-EKF ALGORITHM

In this publication we consider a simple special case of the more general multistage estimator of Figure 4, wherein the first stage is the DLS algorithm of the previous section and the second stage is an extended Kalman filter (EKF). As the dynamic variation of the error signal $\tilde{\Theta}(k) = \Theta^1(k)$ of Figure 4 is much smaller compared to the original signal $\Theta(k)$ (the frequency variation over any update interval is much smaller), the effective averaging time period for the second-stage Kalman filter can be selected to be higher than for the first stage DLS algorithm. This is achieved by selecting a smaller value of the "dynamic noise" covariance matrix Q (see equation (19)) for the EKF and/or a higher value for the exponential data weighting coefficient λ.

Extended Kalman Filter (EKF) Algorithm

Here we consider the problem of estimating the unknown error signal parameters $\omega_{0\ell}$, $\gamma_{0\ell}$ and $\delta_{0\ell}$ in the ℓth VCO update period for any integer $\ell \geq 1$ on the basis of the set of measurements $\{y^1(k), z^1(k)\}$ of equation (22) below (see also Figure 4) by an EKF.

$$\begin{aligned} y^1(k) &= ASin(\Theta^1(k)) + v_i^1(k) \\ z^1(k) &= ACos(\Theta^1(k)) + v_q^1(k) \\ \Theta^1(k) &= \theta_{0\ell} + \omega_{0\ell} jT_s + \gamma_{0\ell}(jT_s)^2 + \delta_{0\ell}(jT_s)^3 \\ k &= N(\ell-1) + j \; ; j = 1, 2, \ldots, N \quad ; \ell = 1, 2, \ldots \end{aligned} \tag{22}$$

Note that as for the DLS algorithm the parameter vector $\psi_{0\ell} = [\theta_{0\ell} \quad \omega_{0\ell} \quad \gamma_{0\ell} \; \delta_{0\ell}]'$ may be different over different VCO update intervals. For computational simplicity we use a third-order EKF and thus ignore the contribution of the last term in the expression for $\Theta^1(k)$ which is appropriate for the GPS trajectories considered here. Denoting the state and parameter vectors at time $k = N(\ell-1) + j$ by $\psi_\ell(j)$ and η_ℓ respectively, i.e., with $\psi(j) = [1 \quad jT_s \quad 0.5(jT_s)^2]'$, $\eta_\ell = [\theta_{0\ell} \quad \omega_{0\ell} \quad 2\gamma_{0\ell}]'$, the extended Kalman filter equations for the update of $\hat{\eta}_\ell$, the estimate of η_ℓ, are given by

$$\hat{\eta}_\ell(j) = \hat{\eta}_\ell(j-1) + K_\ell(j)\nu_\ell(j)$$

$$K_\ell(j) = \sum_\ell(j-1)\psi(j)(\lambda + \psi'(j)\sum_\ell(j-1)\psi(j))^{-1}$$

$$\sum_\ell(j) = \{\sum_\ell(j-1) - \sum_\ell(j-1)\psi(j)[\lambda + \psi'(j)\sum_\ell(j-1)\psi(j)]^{-1}\psi'(j)\sum_\ell(j-1)\}/\lambda \qquad (23)$$

$$\nu_\ell(j) = y^1(k)Cos(\hat{\phi}_\ell(j)) - z^1(k)Sin(\hat{\phi}_\ell(j))$$

$$\hat{\phi}_\ell(j) = \psi'(j)\hat{\eta}_\ell(j-1) \quad ; k = (\ell-1)N + j\,; j = 1, 2\ldots, N; \ell = 1, 2, \ldots$$

In the equations (23) above, the initial estimate $\hat{\eta}_\ell(0)$ is simply taken to be equal to $\hat{\eta}_{\ell-1}(N)$. This is an appropriate choice for the initial estimate in view of the fact that if the first stage of the estimation algorithm is convergent then η_ℓ would be random and remain close to zero for all ℓ. However, if the errors in the previous stage are not close to zero, then the components of η_ℓ would possess some continuous drift term, i.e., $\omega_{0\ell}$ will have a component linear in time if $\gamma_{0\ell} \neq 0$. The "initial error covariance" matrix $\sum_\ell(0)$ is simply set equal to some diagonal matrix representing the uncertainty in the difference parameter $\eta_\ell - \eta_{\ell-1}$.

Estimation in the Presence of Data Modulation

In this case one could apply the more sophisticated version of [9], wherein an explicit detection of possible data transitions is followed by the demodulation of data, thus effectively reducing the problem to the case of no data modulation considered above. However, here we bypass such a detection and instead propose a simple modification in the estimation algorithm that takes into account the data modulation. If the VCO update interval T is selected equal to bit period T_b, then the data modulation represents an additional phase uncertainty at the boundaries of the update intervals. This is taken into account by adding an appropriate value, say $(\pi/2)^2$, to the first diagonal element of $\sum_\ell(0)$ and modifying the initial estimate $\hat{\eta}_\ell(0)$ by $\pi/2$, i.e., $\hat{\eta}_\ell(0) = \hat{\eta}_{\ell-1}(N) + \pi/2$, for those values of ℓ that correspond to bit boundaries. Such an algorithm is expected to result in somewhat higher estimation errors compared to the more sophisticated scheme of [9], but is much simpler in terms of implementation. In this case of a two-stage estimator

(see Figure 4), the estimates of the input signal phase and frequency at time instances ℓT are given by

$$\begin{aligned}\hat{\hat{\Theta}}(\ell T) &= \Theta_L((\ell-1)T+) + \psi'(N)\hat{\eta}_\ell(N) \\ \hat{\hat{\Omega}}(\ell T) &= \Omega_L((\ell-1)T+) + \hat{\omega}_{0\ell} + 2\hat{\gamma}_{0\ell}\cdot(NT_s)\end{aligned} \tag{24}$$

where $\hat{\omega}_{0\ell}$ and $\hat{\gamma}_{0\ell}$ represent the second and third element respectively of $\hat{\eta}_\ell(N)$.

6. SIMULATIONS

In the following we present simulation results obtained when the algorithm is applied to the tracking of phase and frequency for high dynamic GPS receivers [14]. For the purposes of simulation we assume that the pseudo-random code has been removed from the received signal and symbol timing has been acquired. We consider both the cases when the data modulation has also been removed via an auxiliary link [8, 14] and the case when an unknown data modulation is present. For the simulations we consider a sampling rate of 500 samples/second and simulate a high dynamic trajectory considered previously in [14] and reproduced in Figure 5. In Figure 5, the acceleration and the jerk (the derivative of acceleration) are measured in units of g where g is the gravitational constant (equal to 9.8 m/s). In the case when data modulation is present, we assume a BPSK modulation at a rate of 50 bits/second.

The parameters of most interest in this application are the instantaneous phase and frequency of the input signal $r_I(t)$, which corresponds to the high dynamic GPS trajectory of Figure 5. Since we are mainly interested in the tracking performance of the proposed algorithm, we assume as in [14] that the initial trajectory parameters at zero time are known. The received signal carrier frequency $f_c = \omega_c/2\pi$ in the signal model (1) is taken to be equal to 1.575 GHz. The GPS receiver instantaneous pseudo-range R in meters and velocity v_d in m/s are related to the instantaneous phase $\Theta_I(t)$ of (1) and its derivative $\dot{\Theta}_I(t)$ as

$$\begin{aligned} R &= \frac{\Theta}{2\pi}\frac{c}{f_c} \\ v_d &= f_d\frac{c}{f_c} = \frac{\dot{\Theta}}{2\pi}\frac{c}{f_c} \end{aligned} \tag{25}$$

where f_d denotes the Doppler in Hz and c is the speed of light. Denoting by $\hat{R}(\ell)$ and $\hat{f}_d(\ell)$ the estimates for $R(\ell)$ and $f_d(\ell)$ respectively, which denote the range and Doppler of the input trajectory at the end of ℓth update interval, then the performance measures of the estimation algorithm are given by the following sample rms values of the estimation

errors:

$$\tilde{R}_{rms} \triangleq \frac{1}{L}\sqrt{\sum_{\ell=1}^{L}[R(\ell) - \hat{R}(\ell)]^2}$$
$$\tilde{f}_{d,rms} \triangleq \frac{1}{L}\sqrt{\sum_{\ell=1}^{L}[f_d(\ell) - \hat{f}_d(\ell)]^2} \tag{26}$$

where $L = 4000/N$ is the number of update intervals for the entire trajectory. These measures are obtained as a function of P/N_0, where P denotes the received carrier power and N_0 is the one-sided power spectral density of the receiver bandpass noise.

At lower range of (P/N_0) ratio, the receiver may lose frequency lock, in that the frequency errors at times may exceed ± one-half of the sampling frequency f_s or ± 250 Hz. Since the error signals $\epsilon(k)$ of (11) are the same for frequency errors of Δ Hz as for the case of $\Delta + nf_s$ Hz for any signed integer n, the estimator may make frequency estimation errors of nf_s Hz. This situation may be referred to as cycle slipping in the frequency estimator and is akin to the phenomenon of cycle slipping (phase errors equal to multiples of 2π) in the phase-estimators. If there are one or more cycles slipped in frequency, the computed value of $\tilde{f}_{d,rms}$ would be much larger compared to the case when no such cycle slips occur and would be unacceptable. Thus, another important parameter for the performance is the probability of maintaining frequency lock throughout the trajectory denoted P(lock) or the probability of losing the lock $P_L = 1 - P(lock)$. For the purposes of estimating the probability by digital computer simulations, 100 simulation runs are made for each value of P/N_0 of interest and an estimate of P_L is plotted vs the carrier power to noise power spectral density ratio (CNR). The sample rms values of (26) are also averaged over all those simulation runs for which the frequency lock is maintained. It may well be that for sequences that remain under frequency lock, there may be slipping of cycles in the phase estimates. However, even under the presence of such cycle slips, the computation made on the basis of (25)

provides a good estimate of the pseudo-range as evidenced by the simulations. One cycle slip only corresponds to an error of about 0.2 meters in the pseudo-range estimate.

Figures 6-15 present the simulation results for the DLS algorithm and the composite DLS-EKF algorithms presented in the previous sections. The results for the EKF algorithm operating by itself are available in [14] for comparison. For the simulation results a value of λ equal to 0.97 has been selected. The initial covariance matrix $P(0)$ for the DLS algorithm is selected to be a diagonal matrix, with its diagonal elements equal to 2×10^3, 2×10^7 and 2×10^9 respectively, reflecting the possible uncertainty about the parameters. Three different VCO update intervals equal to 5, 10 and 20 sample times have been considered. The matrix Q of (19) is also selected to be a diagonal matrix for convenience, with its consecutive diagonal elements equal to 4×10^3, 2×10^6 and 10^8. The Q matrix represents possible variations in the input signal parameters over an update interval and is arrived at from the consideration of a-priori estimate of the maximum possible value of the highest order derivative (jerk) present in the input trajectory. For the second stage EKF algorithm, the initial covariance matrix $\sum_\epsilon(0)$ is selected to be also a diagonal matrix but with its elements smaller in value than the corresponding elements of the Q matrix, thus effectively resulting in a higher averaging period and smaller estimation errors compared to the DLS algorithm. The selected values of diagonal elements of $\sum_\epsilon(0)$ matrix are equal to 1.0, 10^3 and 10^6 respectively, in the following simulations. From the simulations it appeared to be advantageous, in terms of numerical stability, to periodically reset the covariance matrix P of the DLS algorithm to its initial value. Such a period was selected to be 10 times the VCO update interval.

Figures 6 and 7 present the simulation results for the performance of DLS algorithm while tracking the high dynamic trajectory of Figure 5 in the absence of any data modulation. Figure 6 plots the probability of losing the frequency lock P_L as a function of CNR for two different values of N equal to 10 and 20. As may be inferred from the figure, a value of P_L of less than 0.1 is obtained for CNRs above 23.1 dB which

is defined to be the threshold point of the algorithm. Figure 6 also plots the average number of cycles slipped in the frequency estimation, denoted by $\overline{N}_{cs}$. In defining such a cycle slip, the entire frequency range is divided into disjoint segments of f_s Hz with the first segment extending from $-f_s/2$ to $f_s/2$ Hz. Whenever the frequency estimation error jumps from one such segment to an adjacent one in either direction, a cycle slip is said to occur. Figure 7 plots the rms error in the Doppler estimation as computed from (26) and averaged over all convergent sequences. For a CNR between 25 and 30 dB-Hz, an rms error of 10-20 Hz is obtained that corresponds to a velocity tracking error of 2-4 m/s. Figure 7 also plots the average length $\overline{L}_{cs}$ of a slipped cycle in terms of number of samples. The information about $\overline{N}_{cs}$ and $\overline{L}_{cs}$ is relevant in the case of multistage algorithm. Figures 8 and 9 present the results for the probability of losing lock P_L and the rms estimation error for the DLS algorithm in the presence of data modulation for three different values of N equal to 5, 10 and 20. As may be observed from the figures, the presence of data modulation increases the threshold by only 0.25-0.5 dB compared to the case of no data modulation. The increase in rms frequency estimation error is about 10% due to data modulation.

Figures 10 and 11 present the performance of the composite DLS-EKF algorithm in the absence of data modulation. We observe that corresponding to $N = 5$, the threshold of the algorithm is 22.75 dB-Hz which is slightly smaller than for the DLS algorithm. However, the rms estimation errors are significantly smaller than for the single-stage DLS algorithm. For the CNR range of 25-30 dB-Hz, the rms error in the Doppler estimation lies in the range of 4-15 Hz corresponding to a velocity estimation error range of 0.8 to 3 m/s. The DLS-EKF algorithm also provides the carrier phase estimate. The modulo-2π phase-estimation error is plotted in Figure 12, from which it is clear that the algorithm is capable of coherent data detection with small probability of error if the CNR is higher than 25 dB-Hz. In fact, as shown in Figure 15, the algorithm provides good estimates of pseudo-range (related to the absolute phase error via (25)) up to a

CNR of about 23 dB at which point the rms error is less than 4 m. The rms pseudo range error is less than 1 m for CNRs higher than 25.5 dB-Hz.

The corresponding results for the performance of DLS-EKF algorithm in the presence of data modulation are presented in Figure 13-15. For this case a minimum threshold of 23.8 dB is obtained for $N = 10$ which is about 1 dB higher than for the case of no data modulation. In terms of rms estimation errors, for a CNR range of about 25-30 dB-Hz, the rms frequency estimation error lies in a range of 8-20 Hz corresponding to a velocity error of about 1.5 to 4 m/s. For this case, as is apparent from Figure 15, the pseudo-range estimation errors are also higher and for a CNR range of 25-30 dB-Hz lie in a range of 0.3-6 m. Notice, however, that no sharp threshold is observed in either the frequency or phase estimation errors over the entire range of CNR between 22-30 dB-Hz considered in the simulations.

7. COMPARISON WITH PREVIOUS TECHNIQUES

For the case of no data modulation, we compare the performance of the proposed algorithm with some of the techniques analyzed in [14] in terms of their performance when tracking exactly the same high dynamic trajectory. Compared to a more computation-intensive maximum likelihood estimate (MLE) of [14], we observe that the DLS-EKF algorithm requires about 0.25 dB smaller CNR than MLE in terms of threshold. In terms of rms frequency estimation errors, the MLE achieves an rms error between 8 Hz to 35 Hz at a CNR of 23 dB-Hz depending upon the estimation delay ranging between 30-80 samples (higher delay provides smaller error). The DLS-EKF algorithm provides an error of 35 Hz for a delay of 5 samples at a CNR of 23 dB-Hz. The MLE algorithm does not provide any phase estimate. Compared to single stage EKF algorithm, we observe that the DLS-EKF algorithm is about 1.5-2.0 dB better in terms of threshold depending upon the value of exponential data weighting coefficient and the filter order used in the simulations of [14]. In terms of RMS errors, the performance is similar to that of third order EKF alone. Notice, however, that direct comparison with the results of [14] may be somewhat misleading. This is so because while the DLS-EKF algorithm includes all of the sequences in the computation of rms error above 25.5 dB-Hz, EKF rejects about 5% of the worst sequences, as the probability of losing lock is about .05 at CNR of 25.5 dB-Hz. For the case of cross product AFC loop of [14], the threshold lies in a range of 25-28 dB-Hz depending upon the loop parameters. Thus, the DLS-EKF algorithm is superior by 2-5 dB-Hz compared to AFC loop. AFC loop provides a minimum rms frequency error of 25 Hz at a CNR of 28 dB-Hz compared to a minimum of 5 Hz achieved for the DLS-EKF algorithm for the same CNR. Notice that in an AFC loop, the parameters achieving a relatively low estimation error are different than those yielding low thresholds and thus, a range of loop parameters must be considered for proper comparison. In terms of rms phase error the performance of the DLS-EKF algorithm is similar to EKF alone. In terms of computations the DLS-EKF algorithm of the publi-

cation requires about the same number of computations as for a fourth-order EKF but about twice as many computations as a third-order EKF. The number of computations are at least an order of magnitude smaller than the MLE.

For the case when the data modulation is present, we compare the performance of the DLS-EKF algorithm with the MLE algorithm of [7], where a somewhat less severe GPS trajectory is analyzed. The results of [7] show a marked threshold of about 30 dB-Hz in terms of CNR compared to 24 dB-Hz for the proposed algorithm. Thus, the proposed algorithm results in a 6-dB reduction in terms of threshold compared to previous schemes of the literature. Above threshold both the DLS-EKF and MLE algorithms have similar values for rms range estimation and range rate estimation errors (minor differences result due to differences in the trajectories). In terms of computations both of the algorithms are comparable. In terms of threshold on CNR, the DLS algorithm is very close to the composite DLS-EKF algorithm. However, in terms of rms frequency estimation errors, it has significantly higher estimation errors. In those cases where higher estimation errors are acceptable, one may apply the DLS algorithm by itself, as it requires only one-half of the computations required by the DLS-EKF algorithm.

8. CONCLUSIONS

This publication has presented a novel multistage estimation scheme for the efficient estimation of the phase and frequency of a very high dynamic signal, which may possibly be phase modulated by unknown binary data and is received under relatively low carrier-to-noise power ratio conditions. The proposed scheme is of very general nature and has much wider scope than the applications in this publication. For a very important application considered in this publication, the algorithm has been specialized to have just two stages. The first stage of the estimation scheme is a least-squares algorithm operating upon the differential signal model while the second stage is an extended Kalman filter of third order. For the very high dynamic GPS trajectories, the proposed algorithm has been shown to significantly outperform the previous algorithms of the literature in one or more aspects, including threshold on CNR, estimation errors, availability of phase estimates and thus the estimate of pseudo-range, computational complexity, and flexibility. For the case of no data modulation, the proposed scheme has a threshold that is slightly lower than the more computation-intensive implementation of MLE algorithm. When compared to just the EKF operating by itself, the proposed DLS-EKF scheme provides from about 1.5- to 2-dB reduction in threshold. In comparison to more conventional schemes, such as AFC loops, the performance is even better.

For the case when an unknown data modulation is present, the algorithm provides an improvement of 6 dB in terms of threshold on CNR in comparison to the MLE scheme of [7] specifically proposed for such applications. In addition to phase and frequency estimates, the algorithm can provide estimates of frequency derivative as well, although not presented in this publication. The scheme being of a very general nature, it may be possible to reduce the threshold even further by using a higher dimension for the state vector related to the higher number of terms in the Taylor series expansion in arriving at the signal model for the first stage DLS algorithm. Further improvements

are possible by the application of more optimum sampling techniques as proposed in [11]. The performance may also be improved both in terms of the threshold and the rms estimation errors by increasing the number of stages to three or more.

REFERENCES

[1] Rife, D.C., "Single Tone Parameter Estimation from the Discrete-Time Observations," IEEE Transactions on Information Theory, Vol. IT-20, No. 5, pp. 591-598, September 1974.

[2] Friedland, B., "Optimum Steady-State Positions and Velocity Estimation Using Sampled Position Data," IEEE Transactions on Aerospace and Electronic Systems, Vol. 9, pp. 906-911, November 1973.

[3] Polak, D.R., Gupta, S.C., "Quasi Optimum Digital Phase-Locked Loops," IEEE Transactions on Communications, Vol. 21, pp. 75-82, January 1973.

[4] Tufts, D.W., Kumaresan, R., "Estimation of Frequencies of Multiple Sinusoids: Making Linear Prediction Perform Like Maximum Likelihood," Proceedings of the IEEE, Vol. 70, No. 9, pp. 975-987, September 1982.

[5] Friedlander, B., "On the Cramer-Rao Bound for Time Delay and Doppler Estimation," IEEE Transactions on Information Theory, Vol. IT-30, No. 3, pp. 575-580, May 1984.

[6] Abatzoglou, T.J., "A Fast Maximum Likelihood Algorithm for Frequency Estimation of a Sinusoid Based on Newton's Method," IEEE Transactions on Acoustics, Speech and Signal Processing, Vol. ASSP-33, No. 1, pp. 77-89, February 1985.

[7] Hurd, W.J., Statman, J.I. and Vilnrotter, V.A., "High Dynamic GPS Receiver Using Maximum Likelihood Estimation and Frequency Tracking," IEEE Trans. AES Vol. 23, No. 5, pp. 425-437, September 1987.

[8] Hoefener, C.E. and Wells, L., "Utilizing GPS for Ultra-High Dynamic Vehicle Tracking in Space," Proceedings of the International Telemetering Conference, Las Vegas, pp. 771-773, October 1986.

[9] Kumar, R., "Efficient Detection and Signal Parameter Estimation with Applications to High Dynamic GPS Receivers," JPL Publication 88-42, National Aeronautics and

Space Administration, Jet Propulsion Laboratory, California Institute of Technology, Pasadena, CA, December 1988.

[10] Kumar, R., "Fast Frequency Acquisition via Adaptive Least Squares Algorithm," Proceedings of the International Telemetering Conference, Las Vegas, pp. 91-101, October 1986.

[11] Kumar, R., "Differential Sampling for Fast Frequency Acquisition via Adaptive Extended Least Squares Algorithm," Proceedings of the International Telemetering Conference, San Diego, pp. 191-201, October 1987.

[12] Kumar, R. and Hurd, W.J., "A Class of Optimum Digital Phase-Locked Loops," Proceedings of the 25th IEEE Conference on Decision and Control, Athens, Greece, December 1986 .

[13] Kumar, R. and Hurd, W.J., "Fixed Lag Smoothers for Carrier Phase and Frequency Tracking," Proceedings of the IASTED International Symposium on Applied Control and Identification, pp. 160-166, December 1986, also submitted to IASTED Journal. See also, "Optimum Filters and Smoothers Design for Carrier Phase and Frequency Tracking," JPL Publication 87-10, National Aeronautics and Space Administration, Jet Propulsion Laboratory, California Institute of Technology, Pasadena, CA, May 1987.

[14] Vilnrotter, V.A., Hinedi, S. and Kumar, R., "A Comparison of Frequency Estimation Techniques for High Dynamic Trajectories," JPL 88-21, Jet Propulsion Laboratory, California Institute of Technology, Pasadena, CA, September 1988.

[15] Mohanty, N., Random Signals Estimation and Identification, Van Nostrand, 1986.

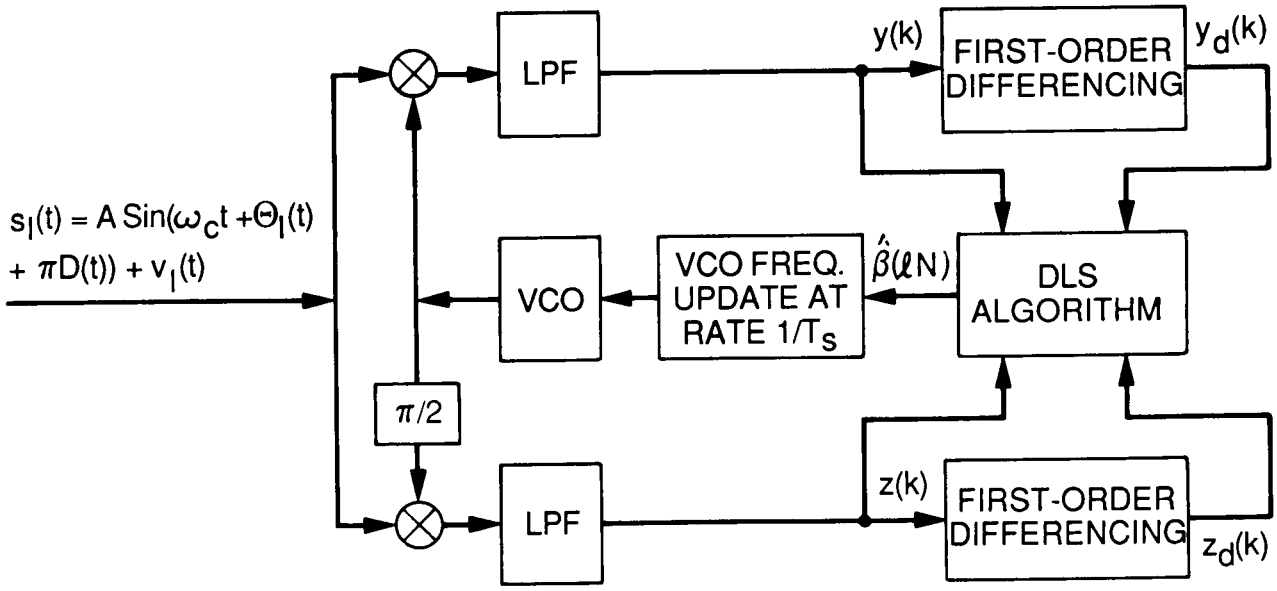

Figure 1. Signal Parameters Estimation by DLS Algorithm

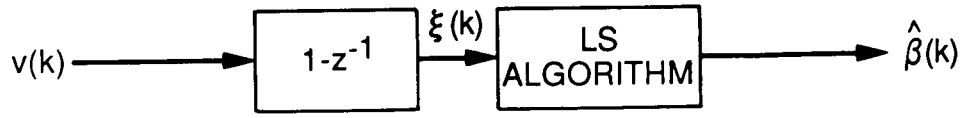

(a)

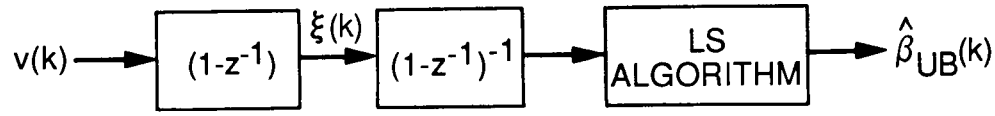

(b)

(c)

Figure 2. LS Algorithms (a) LS Algorithm With Model Noise Colored (b) LS Algorithm With Prewhitened Noise -- Conceptual (c) An Approximate and Realizable Equivalent of (b)

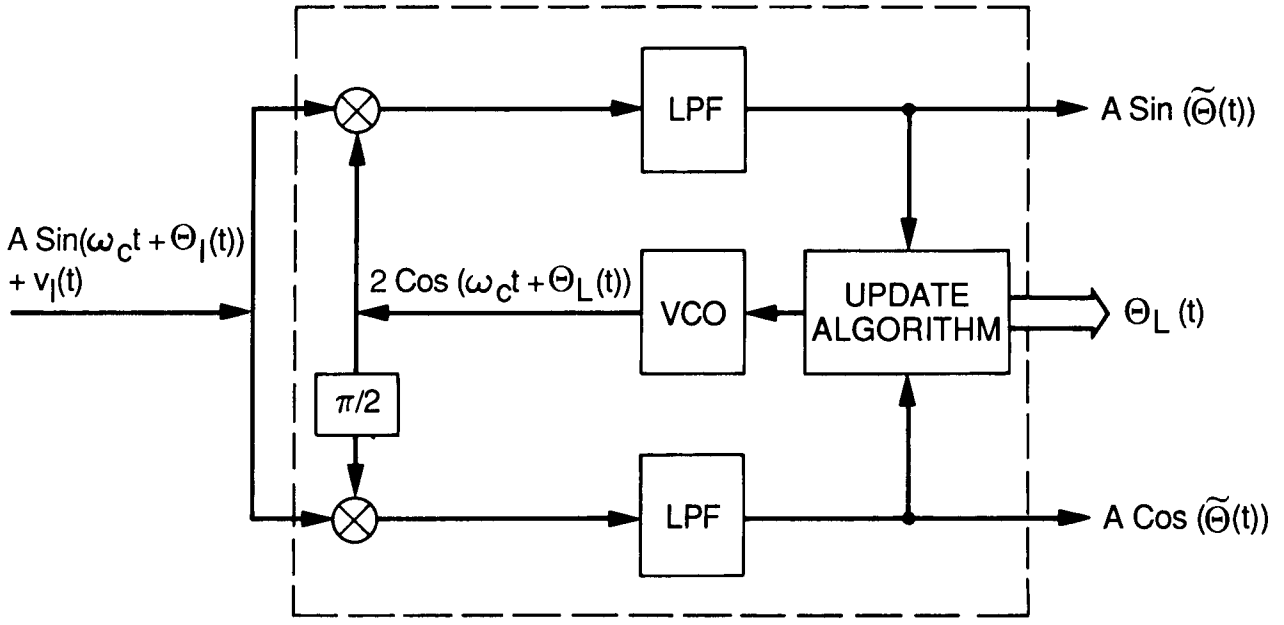

(a)

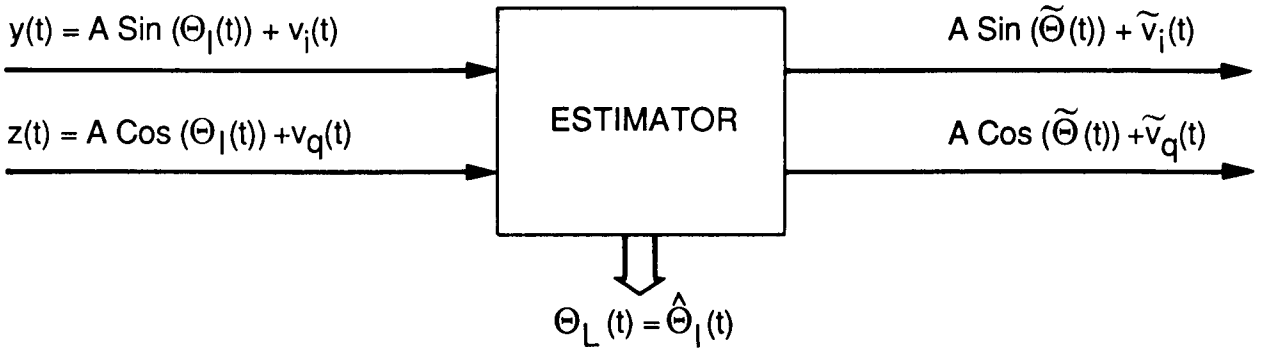

(b)

Figure 3. Single-Stage Estimators (a) A Generalized Single-Stage Estimator (b) An Equivalent Form of Single-Stage Estimator

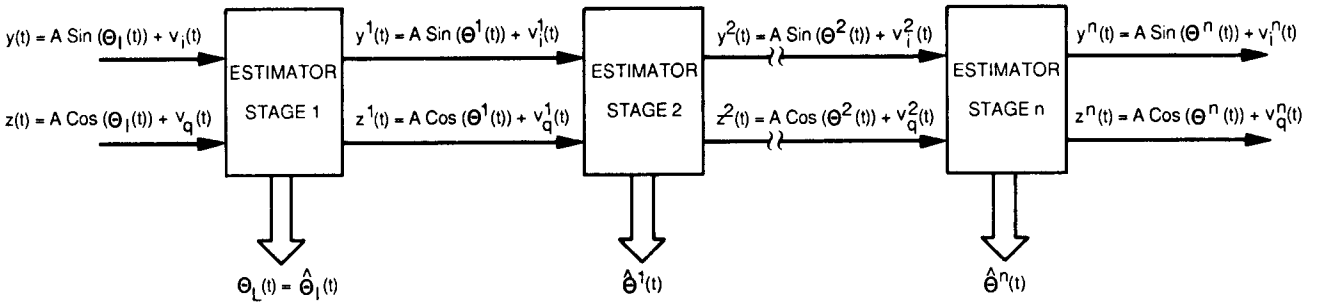

Figure 4. A Multistage Estimator for the Process $\Theta_I(t)$

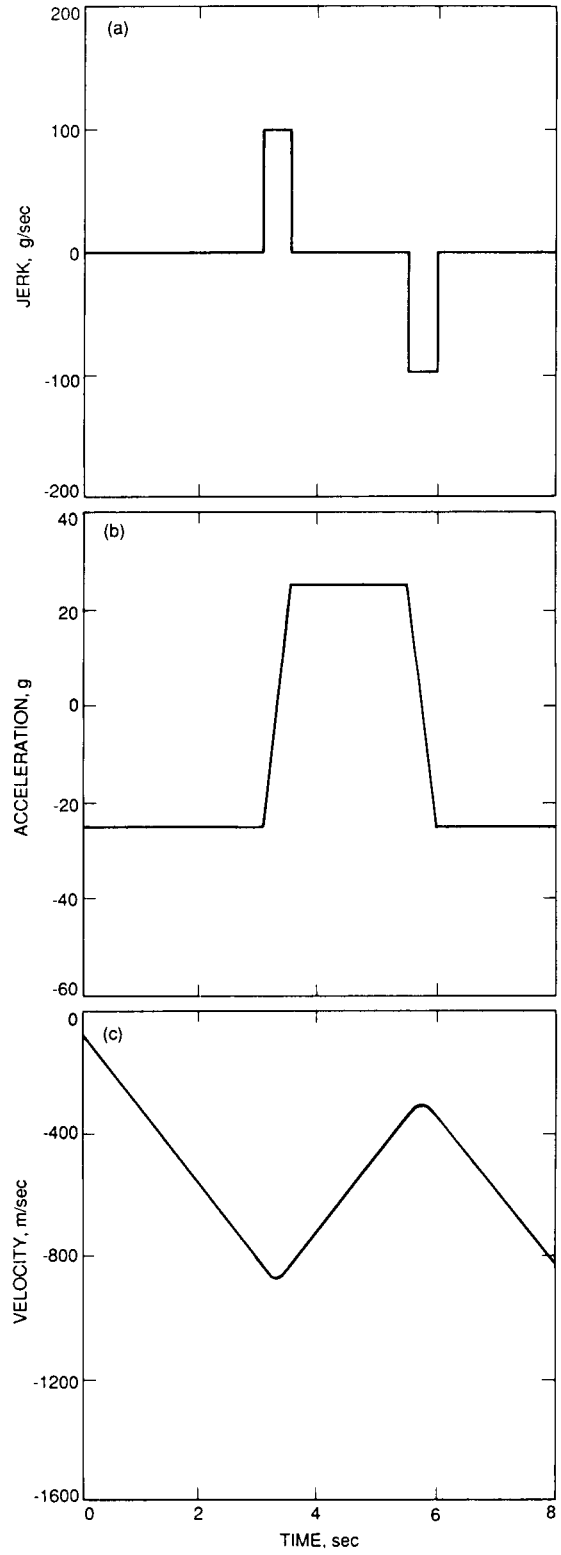

Figure 5. Simulated Trajectory

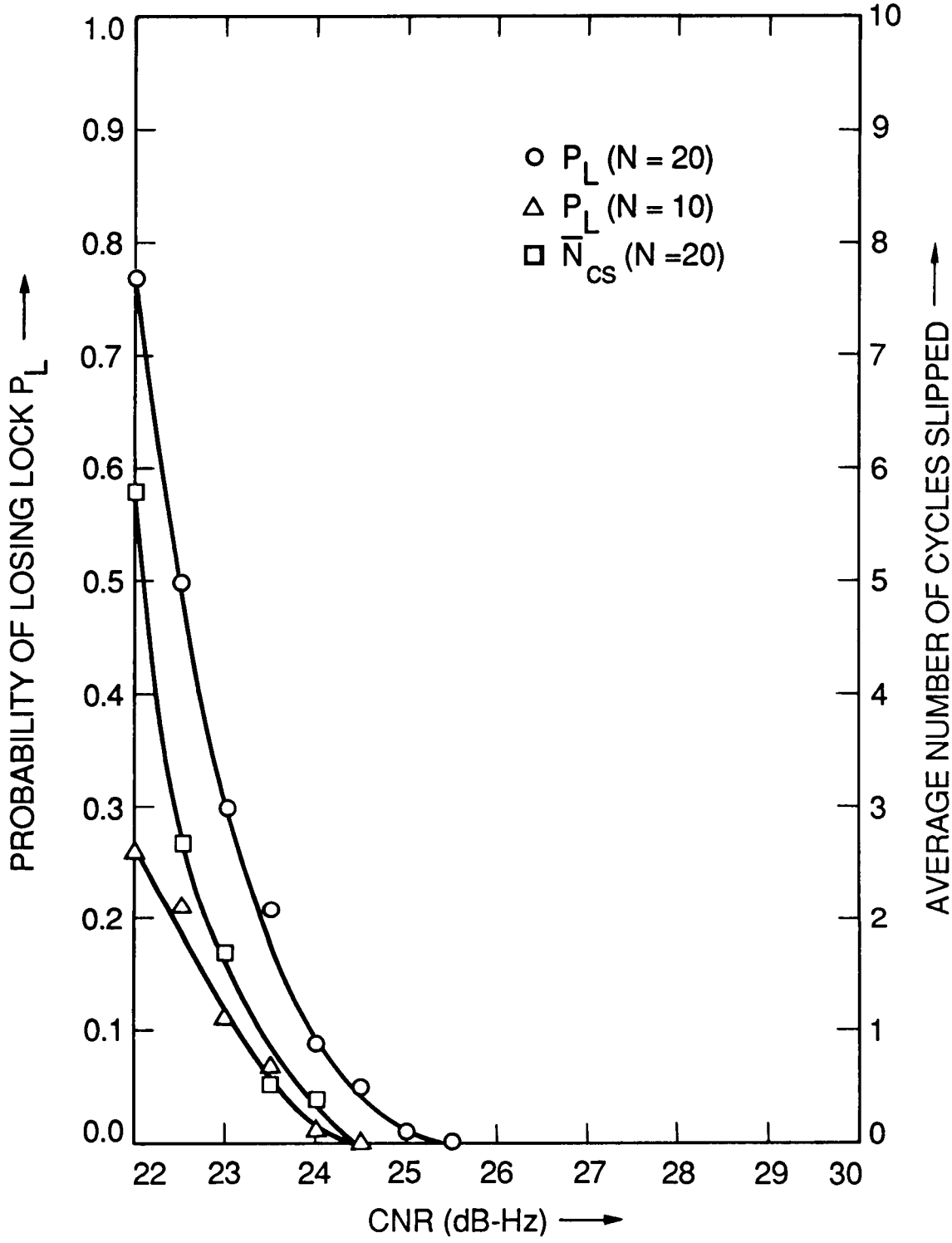

Figure 6. Probability of Losing Frequency Lock vs CNR; DLS Algorithm in the Absence of Data Modulation

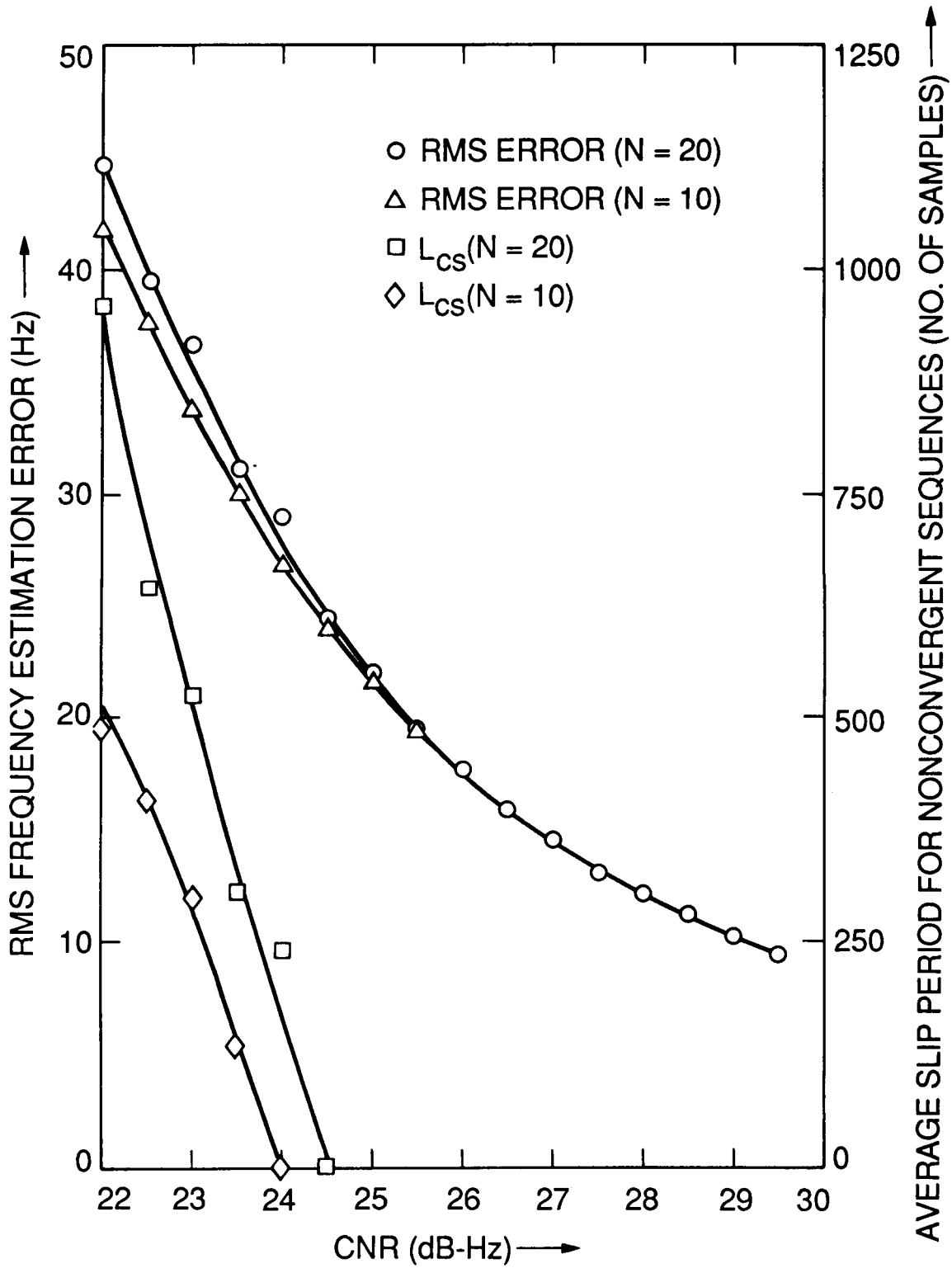

Figure 7. RMS Frequency Estimation Error vs CNR; DLS Algorithm in the Absence of Data Modulation

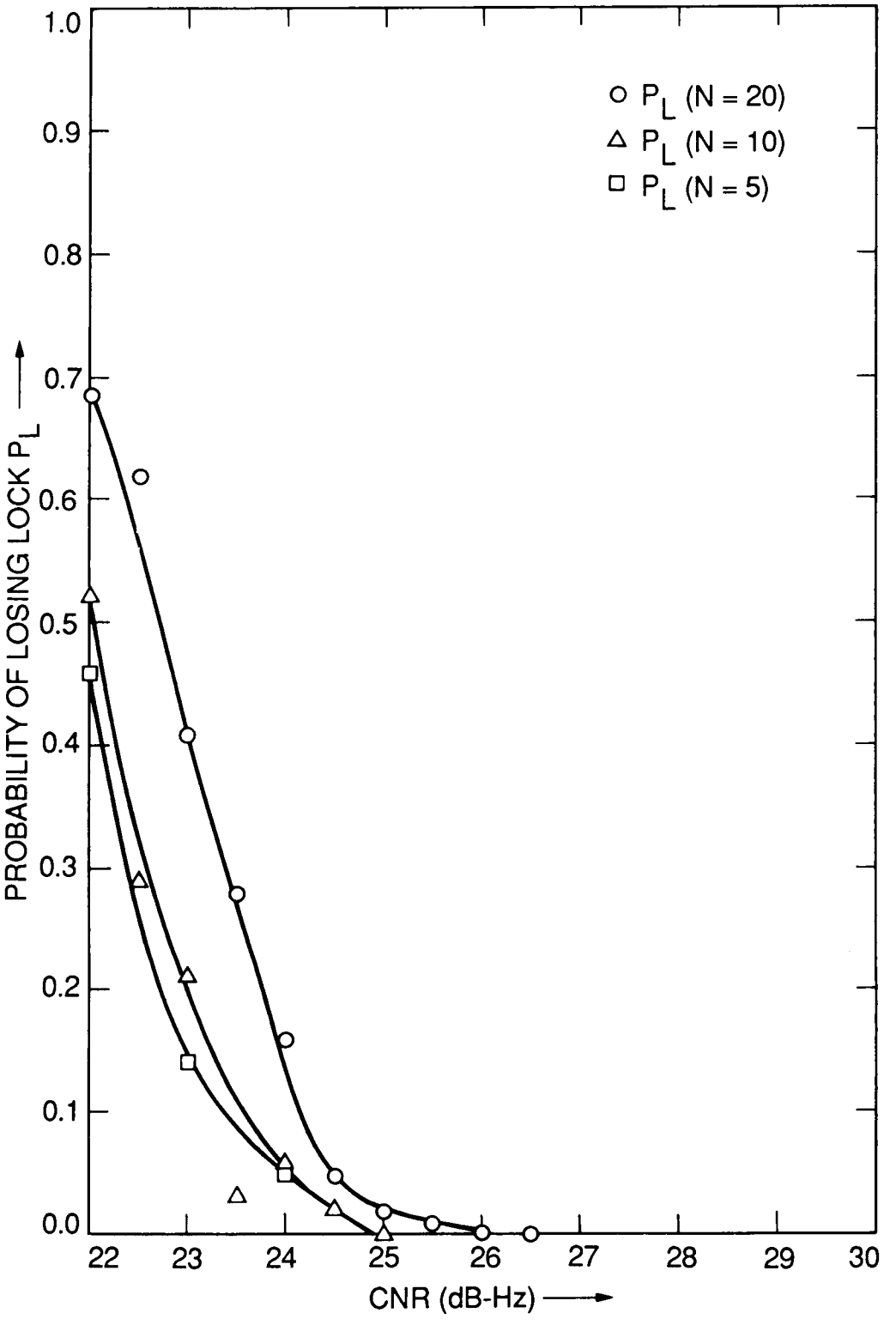

Figure 8. Probability of Losing Frequency Lock vs CNR; DLS Algorithm in the Presence of Data Modulation

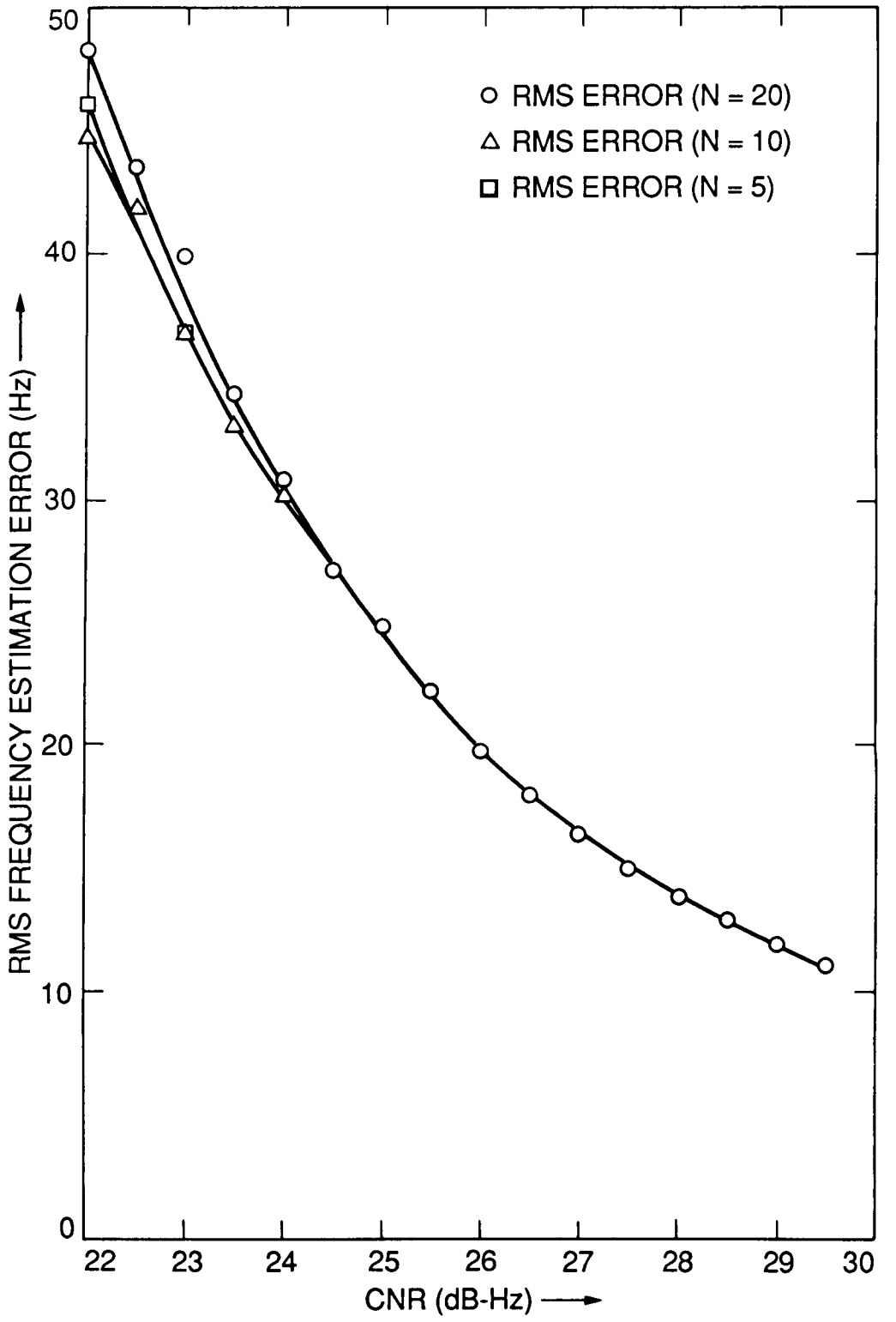

Figure 9. RMS Frequency Estimation Error vs CNR; DLS Algorithm in the Presence of Data Modulation

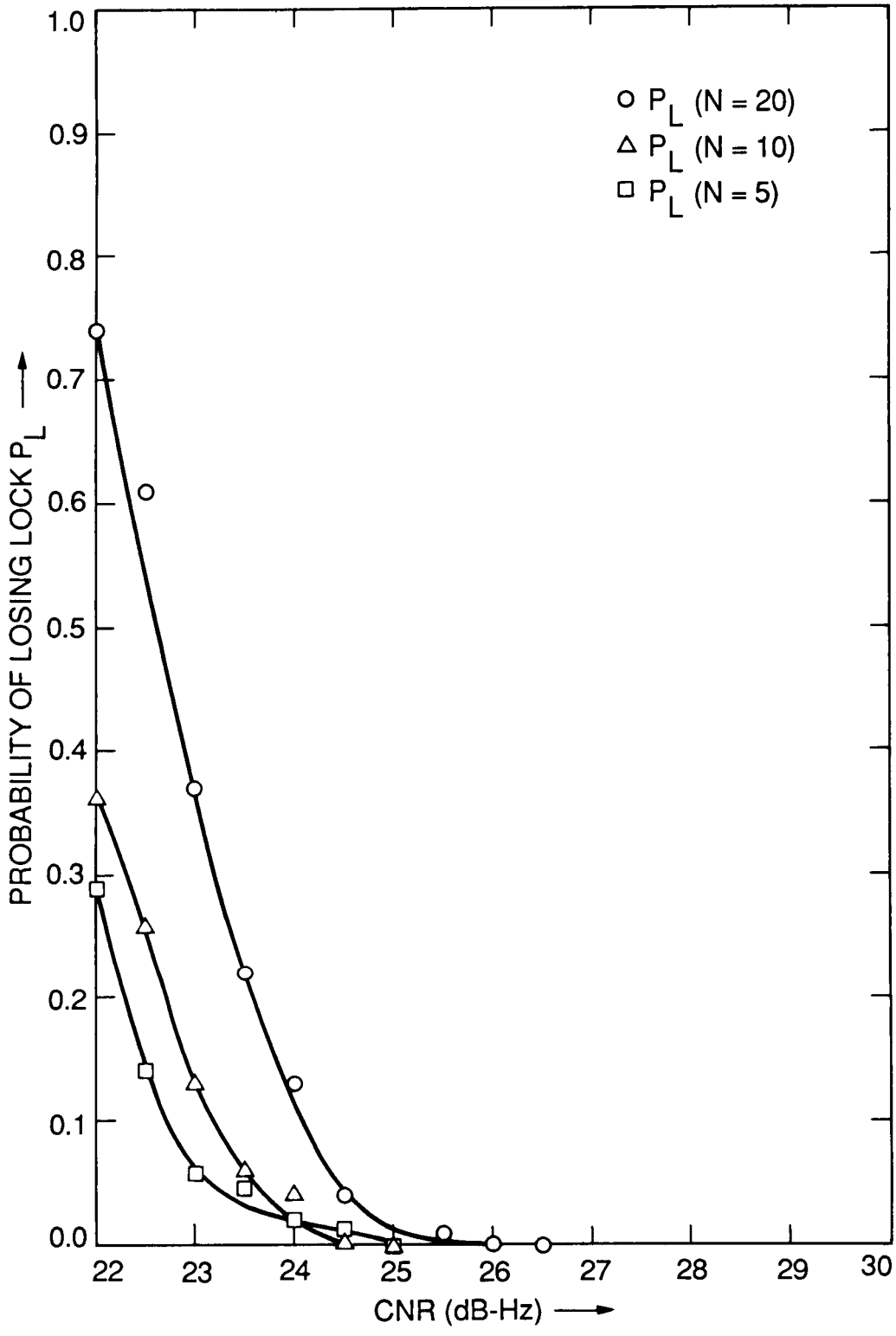

Figure 10. Probability of Losing Frequency Lock vs CNR; DLS-EKF Algorithm in the Absence of Data Modulation

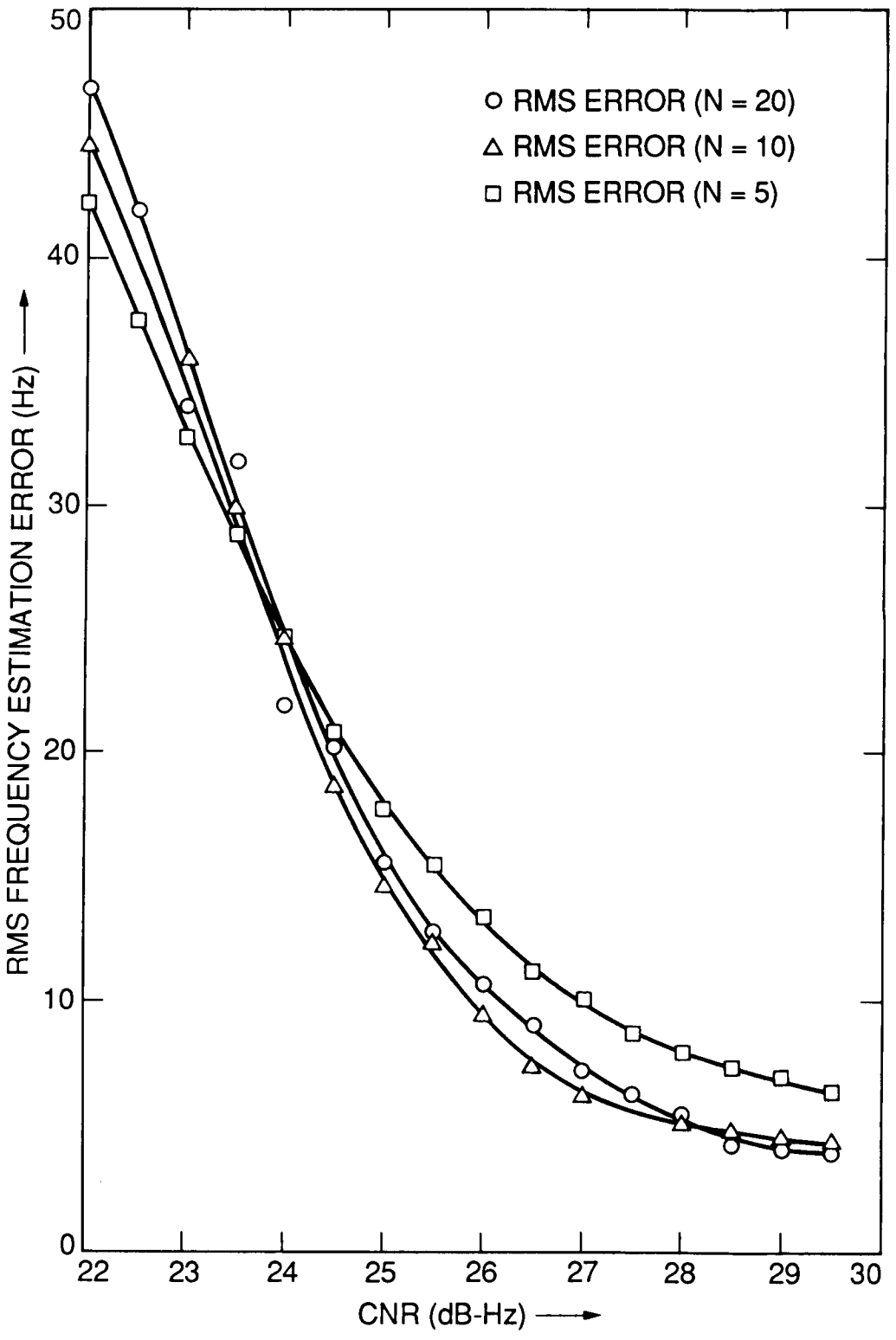

Figure 11. RMS Frequency Estimation Error vs CNR; DLS-EKF Algorithm in the Absence of Data Modulation

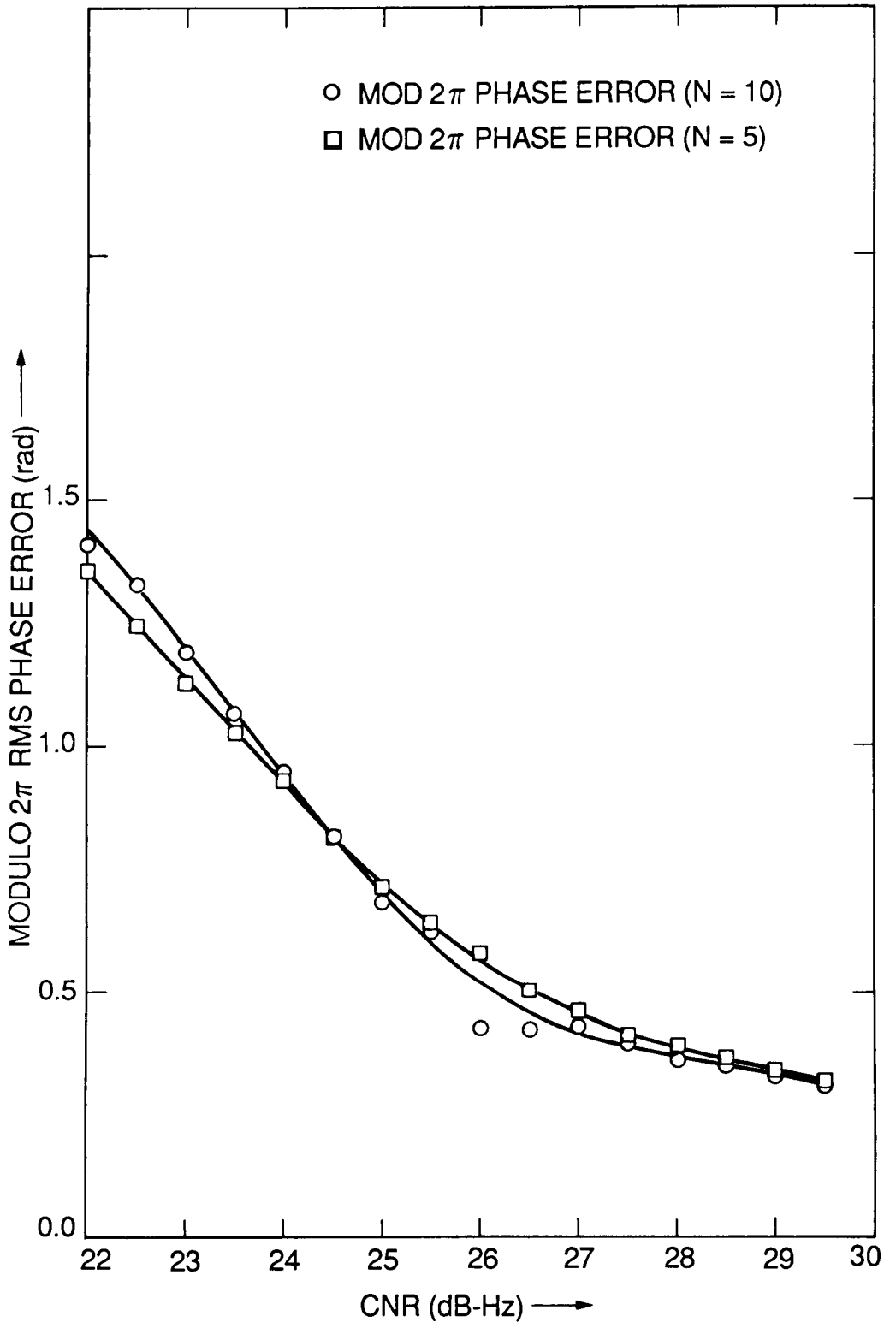

Figure 12. Modulo 2π RMS Phase Error vs CNR; DLS-EKF Algorithm in the Absence of Data Modulation

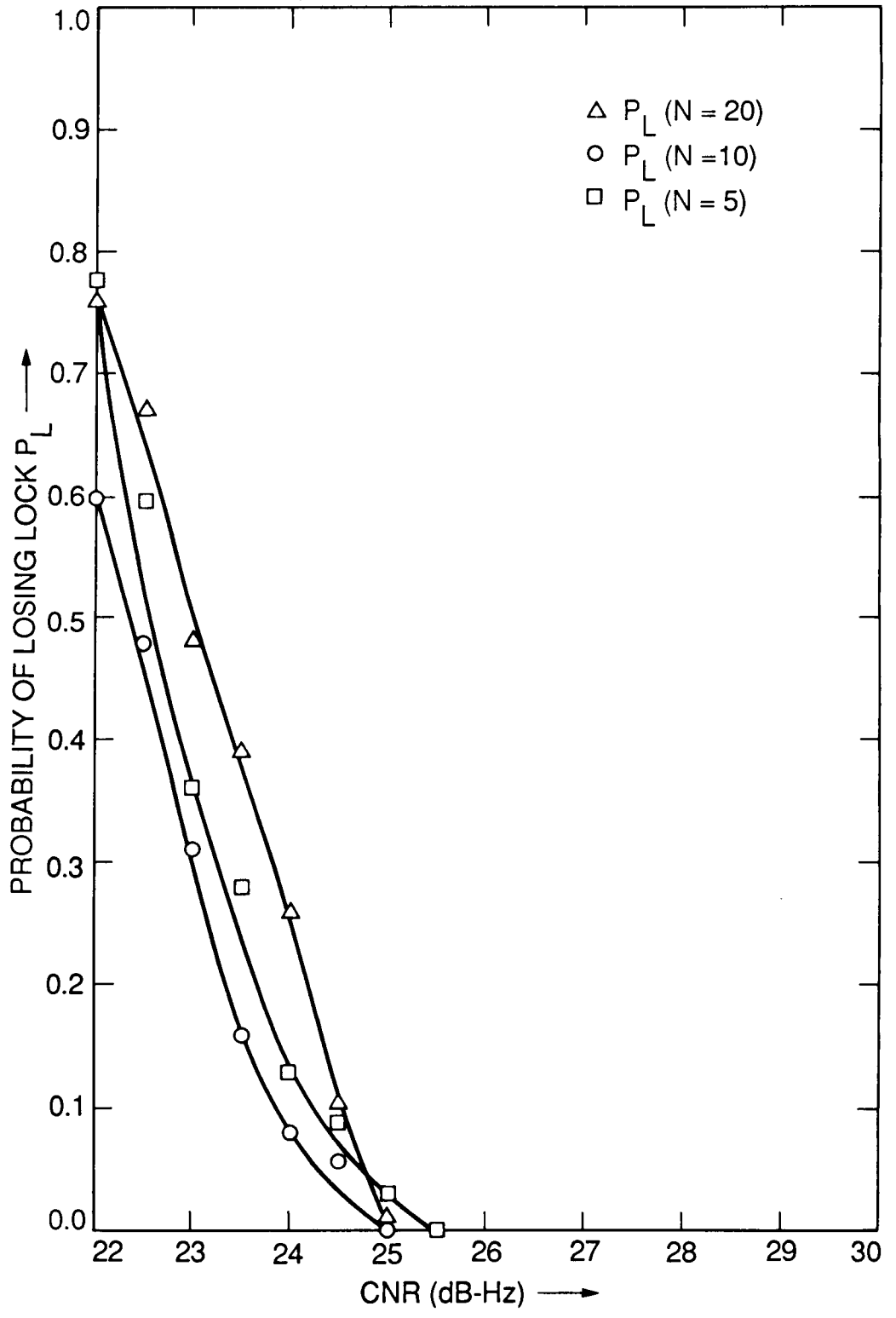

Figure 13. Probability of Losing Frequency Lock vs CNR; DLS-EKF Algorithm in the Presence of Data Modulation

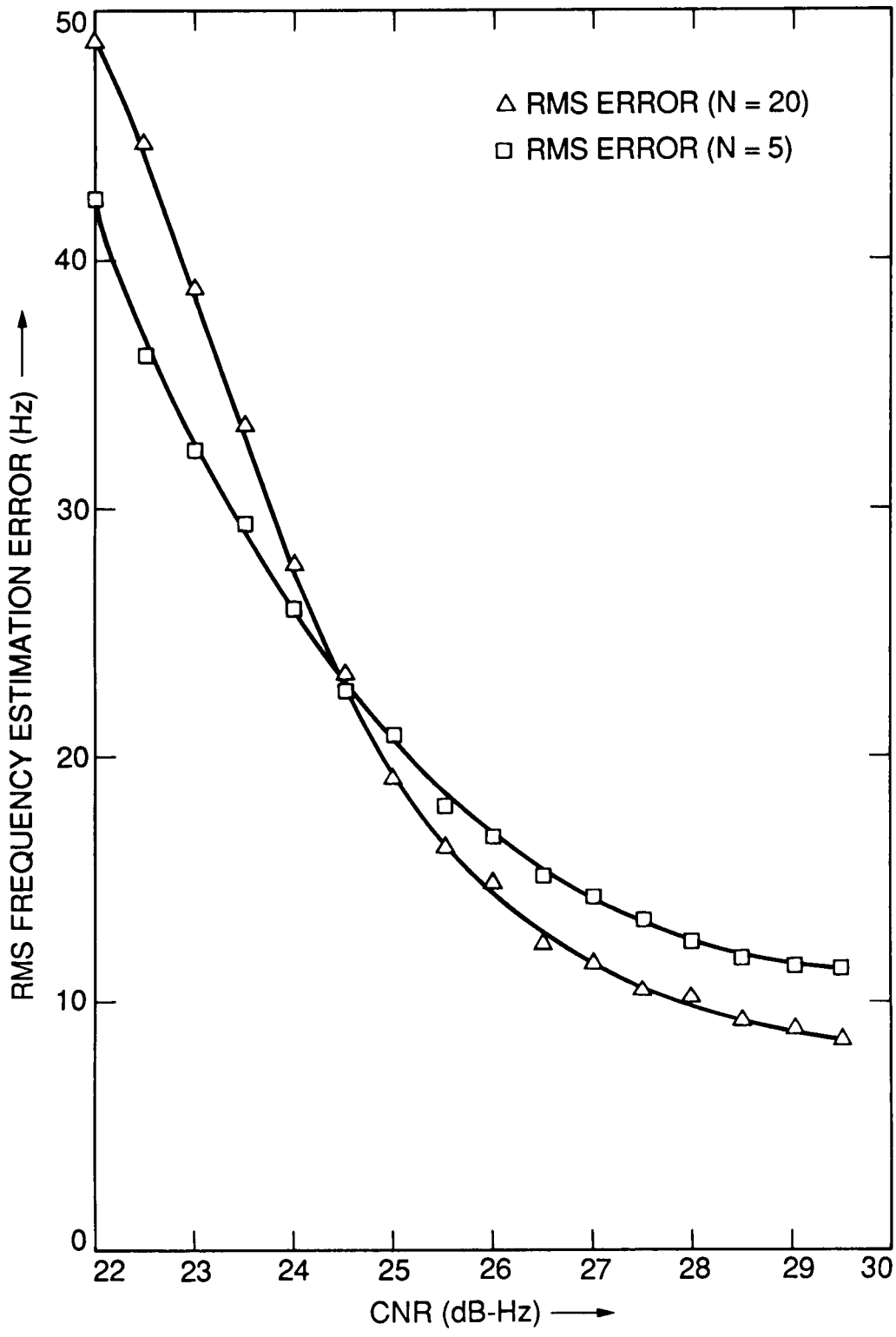

Figure 14. RMS Frequency Estimation Error vs CNR; DLS-EKF Algorithm in the Presence of Data Modulation

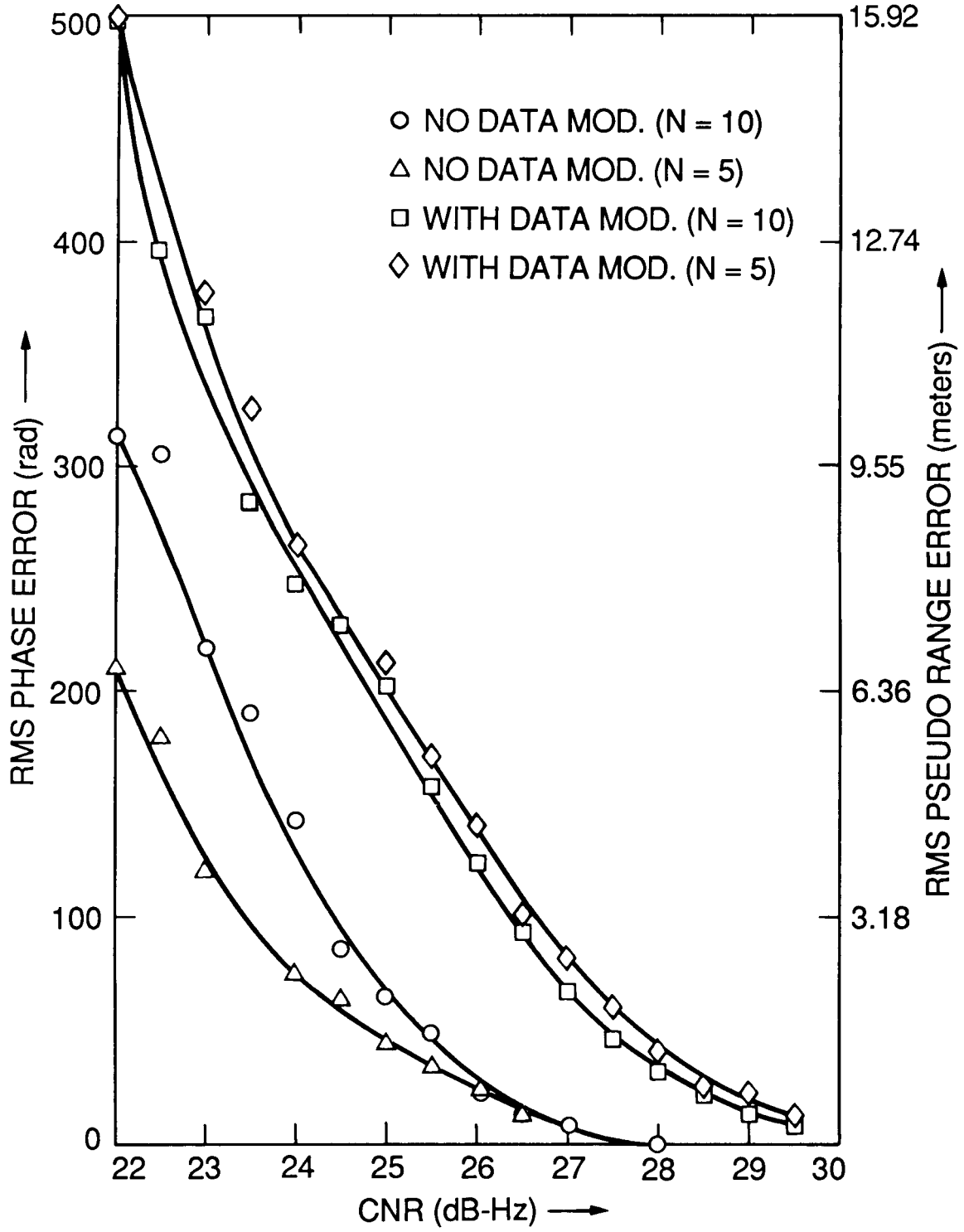

Figure 15. RMS Pseudo-Range Estimation Error vs CNR for DLS-EKF Algorithm; (With and Without Data Modulation)